Nb-1Zr L-PBF In-situ Alloying and Elevated Temperature Mechanical Performance

Eric Brizes [a]

Elizabeth Young-Dohe [a]

Justin Milner [a]

[a] NASA Glenn Research Center, Cleveland, OH

TMS 2024. Orlando, FL. March 3-7

Introduction

- Nb-1Zr is a readily fabricable, dispersion-strengthened Nb alloy with improved elevated temperature properties compared to pure Nb. This alloy is desirable in thermal management systems for fission power and propulsion applications; however, pre-alloyed spherical feedstock is generally unavailable.
- In this work, L-PBF in-situ alloying of a Nb-1Zr chemistry was performed using a high-purity Nb feedstock blended with 1 wt% of Zr-based ceramic nano-powders. The printed material was mechanically tested at room and elevated temperatures in the as-built condition.
- Examination of microstructure and mechanical properties determined the Zr-compound addition with performance most like wrought Nb-1Zr, and the overall feasibility of the in-situ alloying approach.

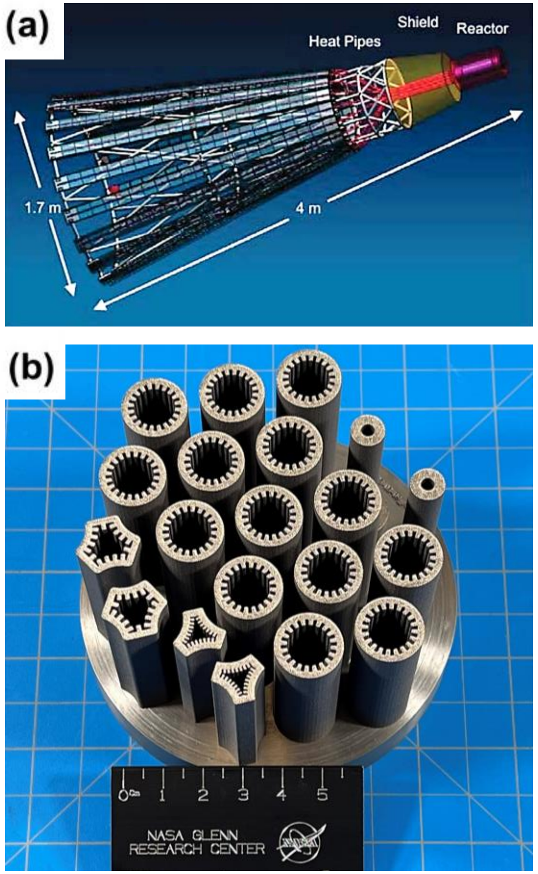

(a) Fission power system 1-kWe (b) printed Nb alloy heat pipe sections

Materials and Powder Processing

- Heritage Barstock
  - Wrought Nb-1Zr (recrystallized)
- L-PBF Powder Feedstock
  - 99.9% Spherical Niobium
    - D_{10} = 21.1 μm
    - D_{90} = 50.4 μm
- Ceramic Nanoparticles
  - **ZrO_2** (20 – 40 nm)
  - **ZrC** (20 nm)
  - **ZrH_2** (1 – 5 μm)

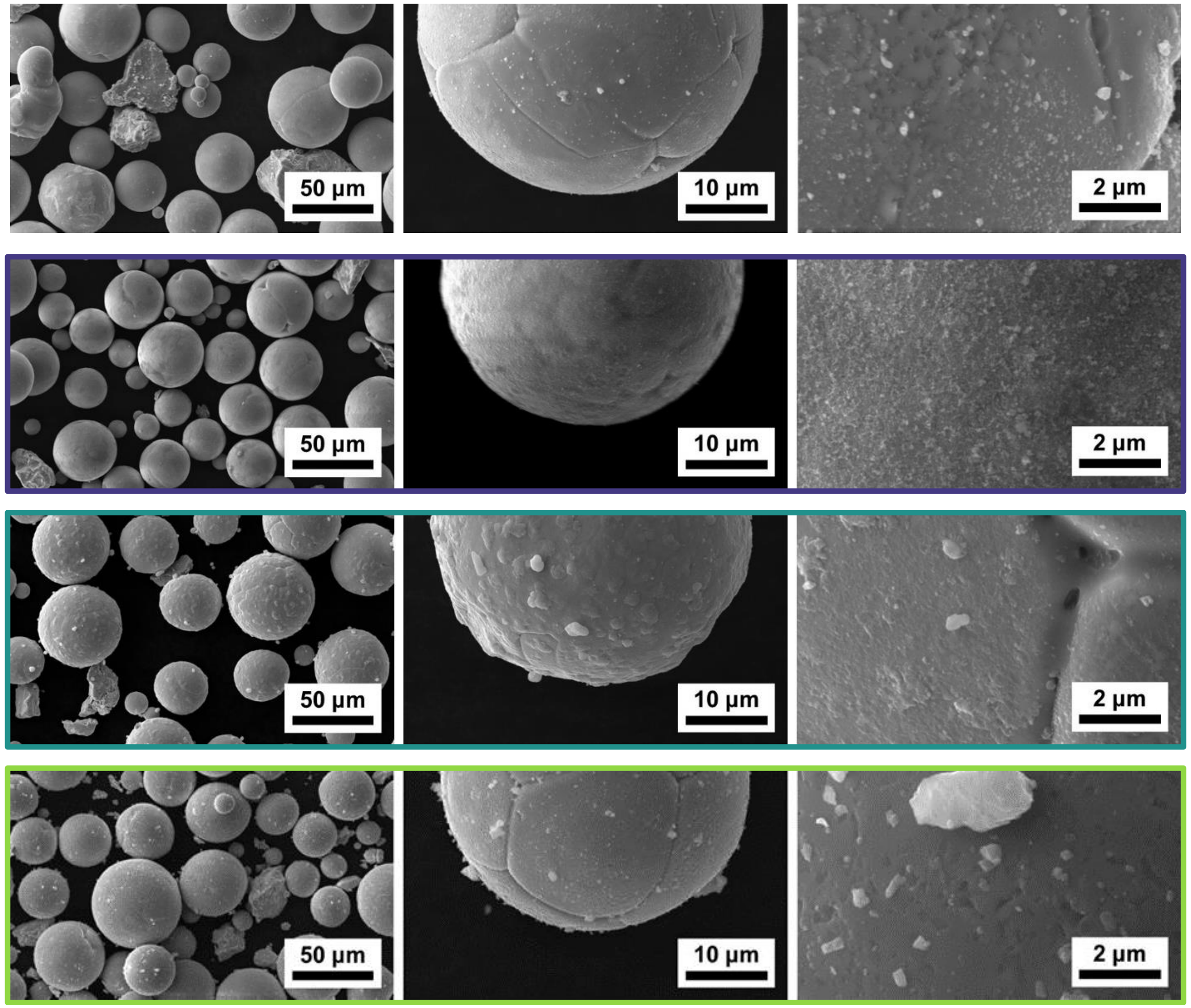

Laser Powder Bed Fusion

- *EOS M100*, 205 J/mm^3, < 10 ppm O_2

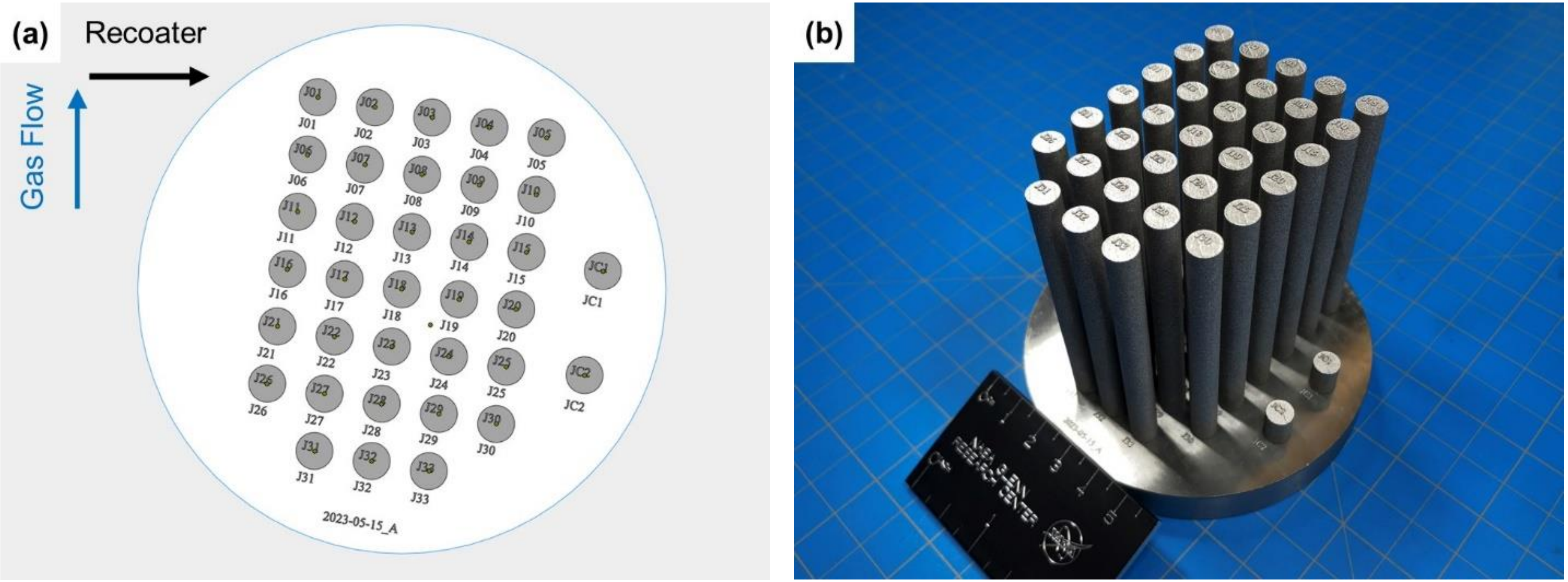

(a) Layout of specimens on the build plate and (b) The as-built specimens

Relative Density

- Determined via image analysis

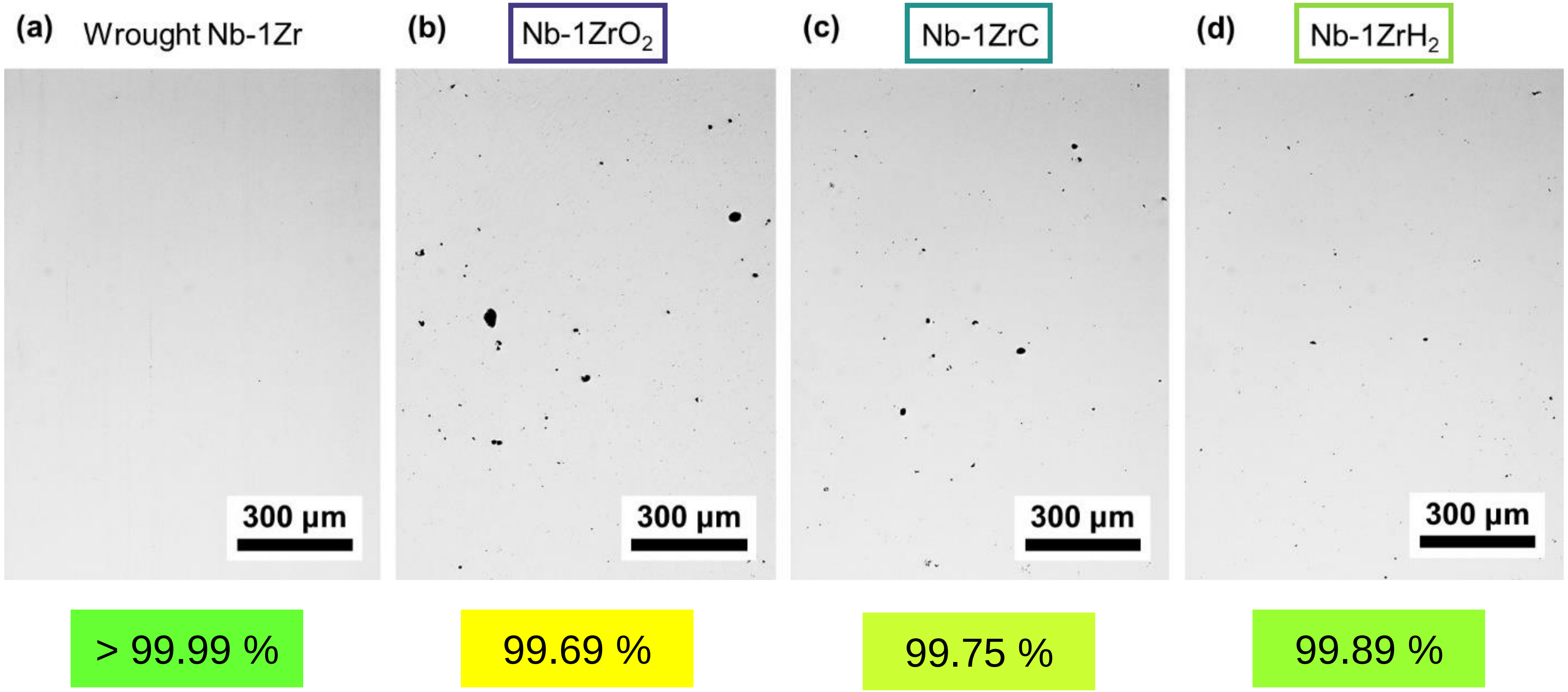

Examples of optical micrographs from which image analysis determined (a) wrought Nb-1Zr, (b) Nb-$1ZrO_2$, (c) Nb-1ZrC, and (d) Nb-$1ZrH_2$ material relative density

Chemical Composition

- Determined via ICP-MS and LECO Combustion analysis

Material	Nb [wt%]	Zr [wt%]	O [ppm]	N [ppm]	C [ppm]
Std. ATSM B391 (max.)	Bal.	0.8-1.2	250	100	100
Wrought	Bal.	0.97	250	119	18
Nb Powder	Bal.	-	660	120	26
Nb-1ZrO_2	Bal.	0.65	2815	232	33
Nb-1ZrC	Bal.	0.43	1094	294	576
Nb-1ZrH_2	Bal.	0.83	695	278	35

A dash symbolizes a result of “not detected”

Hammer Bend Screening Test

- Specimen Dimensions: 70 x D7 mm

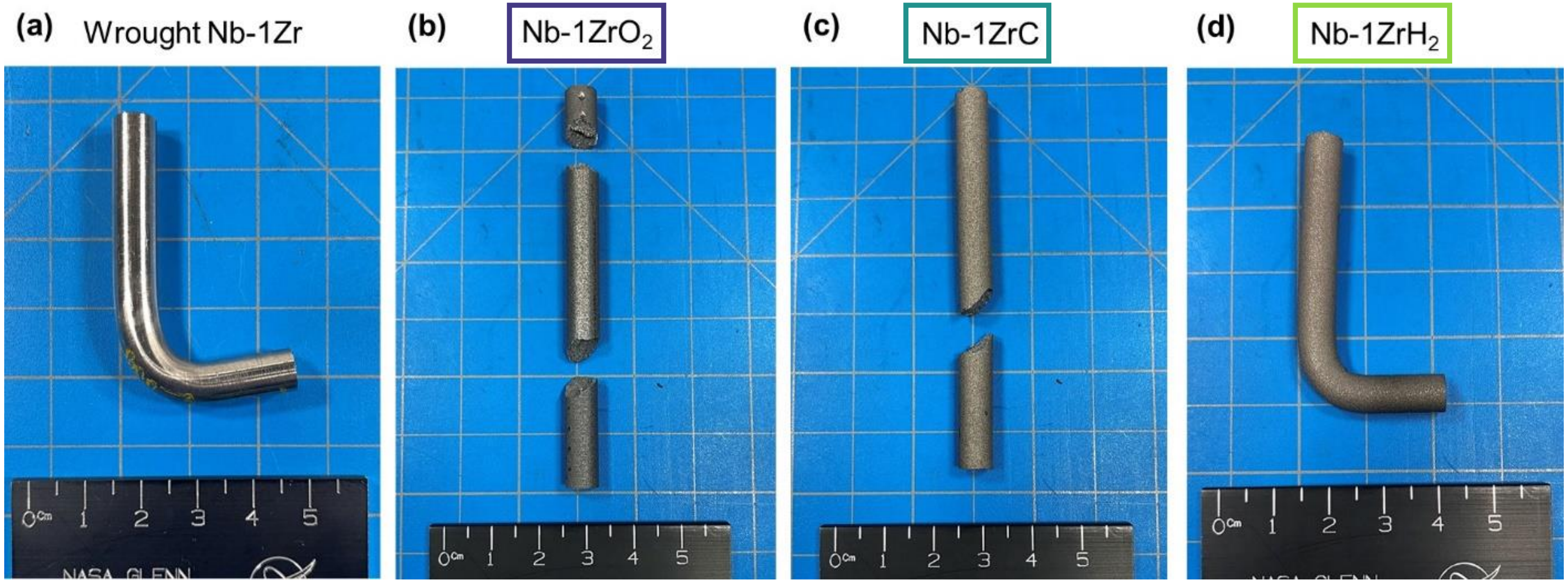

Specimens were secured in a vise and beat with a hammer until failure or the completion of a 90-degree bend

Room Temperature [AIR] Tensile Testing

- 2 tests each at 20ºC per ASTM E8/E8M, strain via laser extensometer

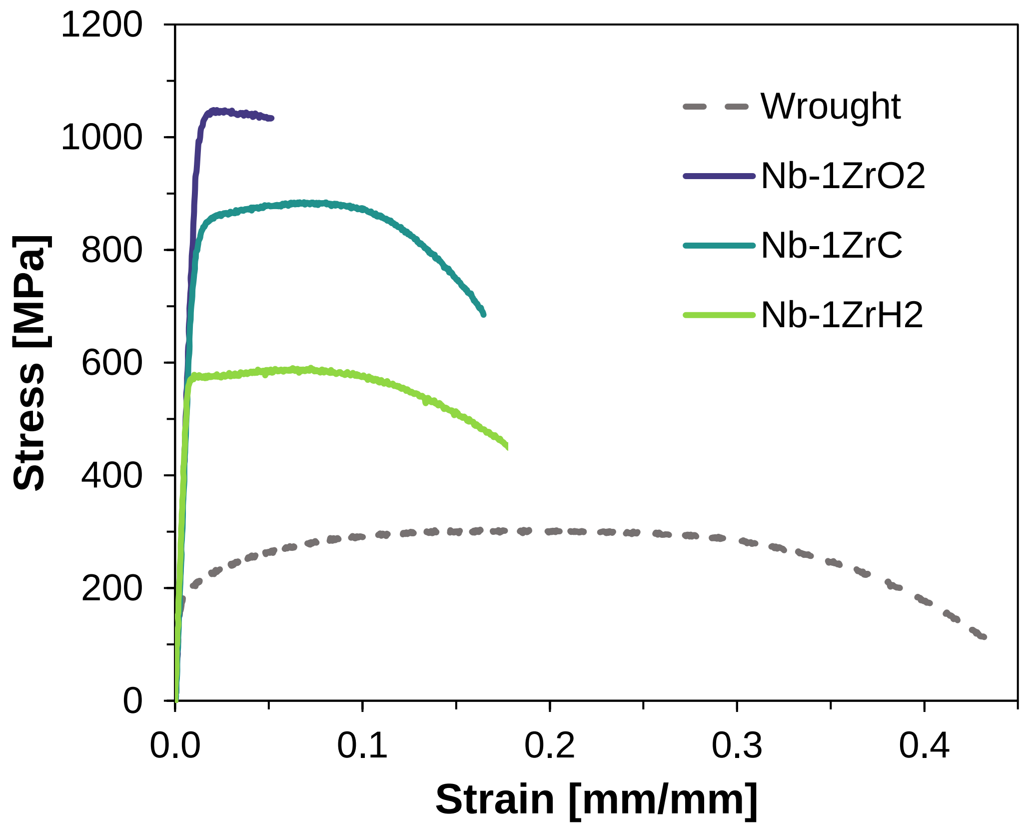

Material	20 °C			
	EM [GPa]	YS [MPa]	UTS [MPa]	El. [%]
Wrought	74.6	184	304	44
Nb-1ZrO$_2$	95.1	989	1034	7
Nb-1ZrC	89.6	802	891	18
Nb-1ZrH$_2$	86.8	566	585	20

Elevated Temperature [VACUUM] Tensile Testing

- 1 test each at 1300ºC per ASTM E21, < 1E-4 Pa, strain via crosshead displacement

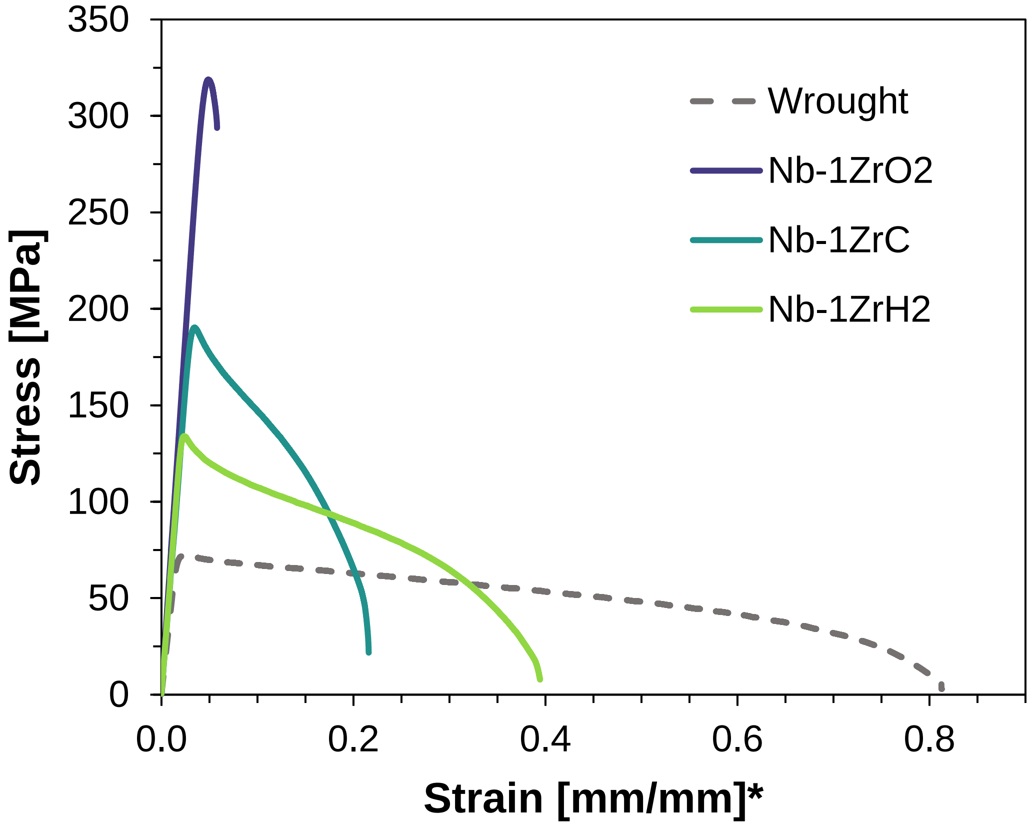

Material	1300 °C			
	EM [GPa]*	YS [MPa]	UTS [MPa]	El. [%]
Wrought	20.7	69	72	81
Nb-1ZrO$_2$	34.1	307	319	6
Nb-1ZrC	30.7	187	190	22
Nb-1ZrH$_2$	30.0	133	134	40

*Estimated due to crosshead displacement strain acquisition

Fractography

- Fracture regions outlined in a yellow-dotted line

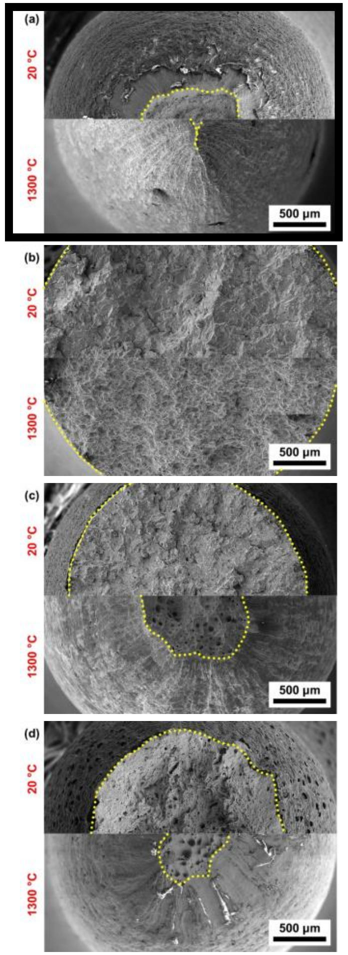

Wrought

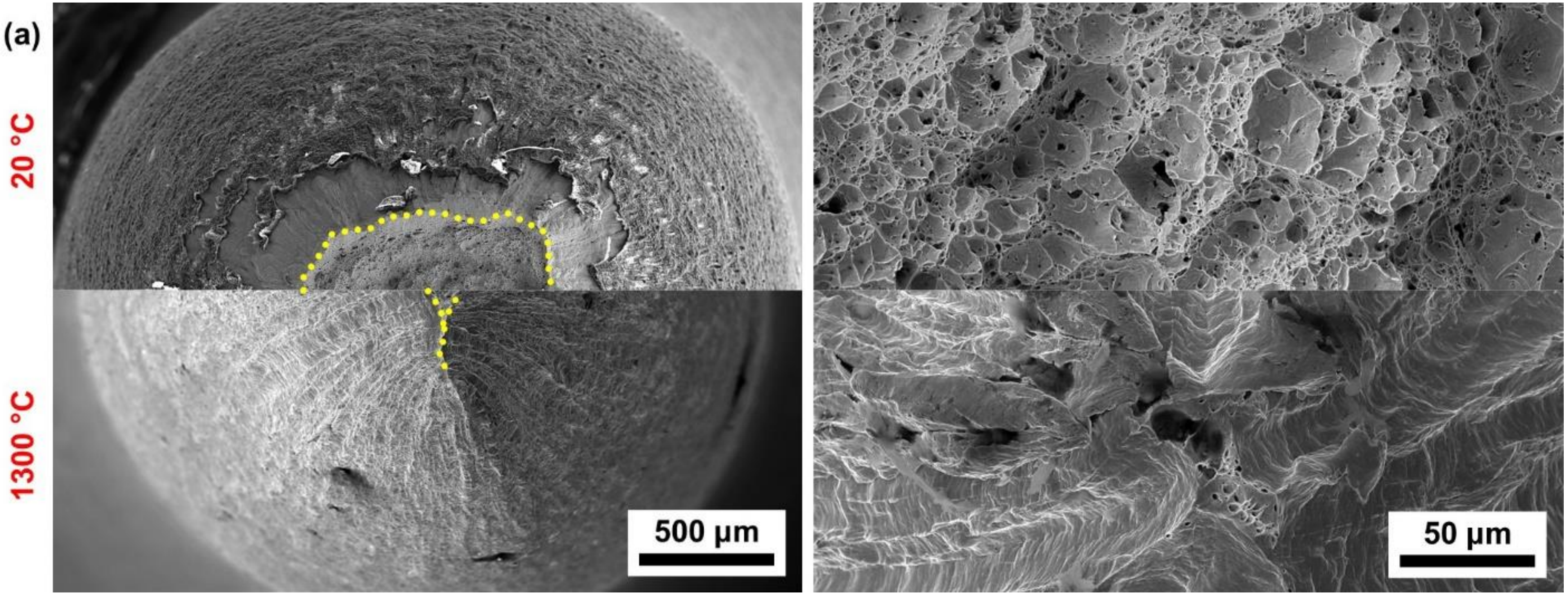

Low (200 X) and high (2 kX) magnification secondary electron images

Fractography

- Fracture regions outlined in a yellow-dotted line

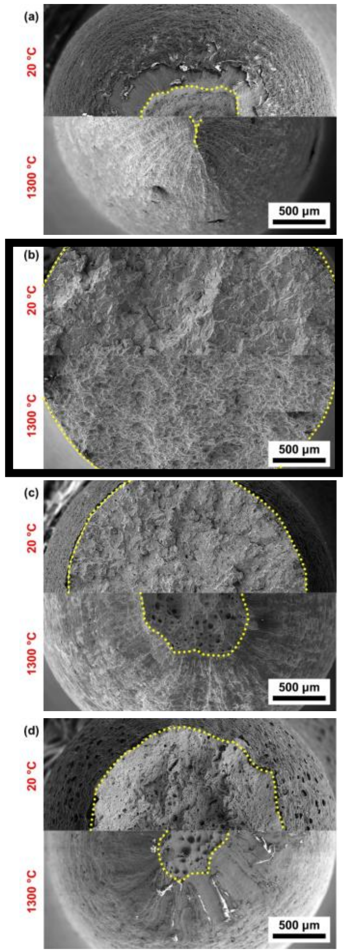

Nb-1ZrO$_2$

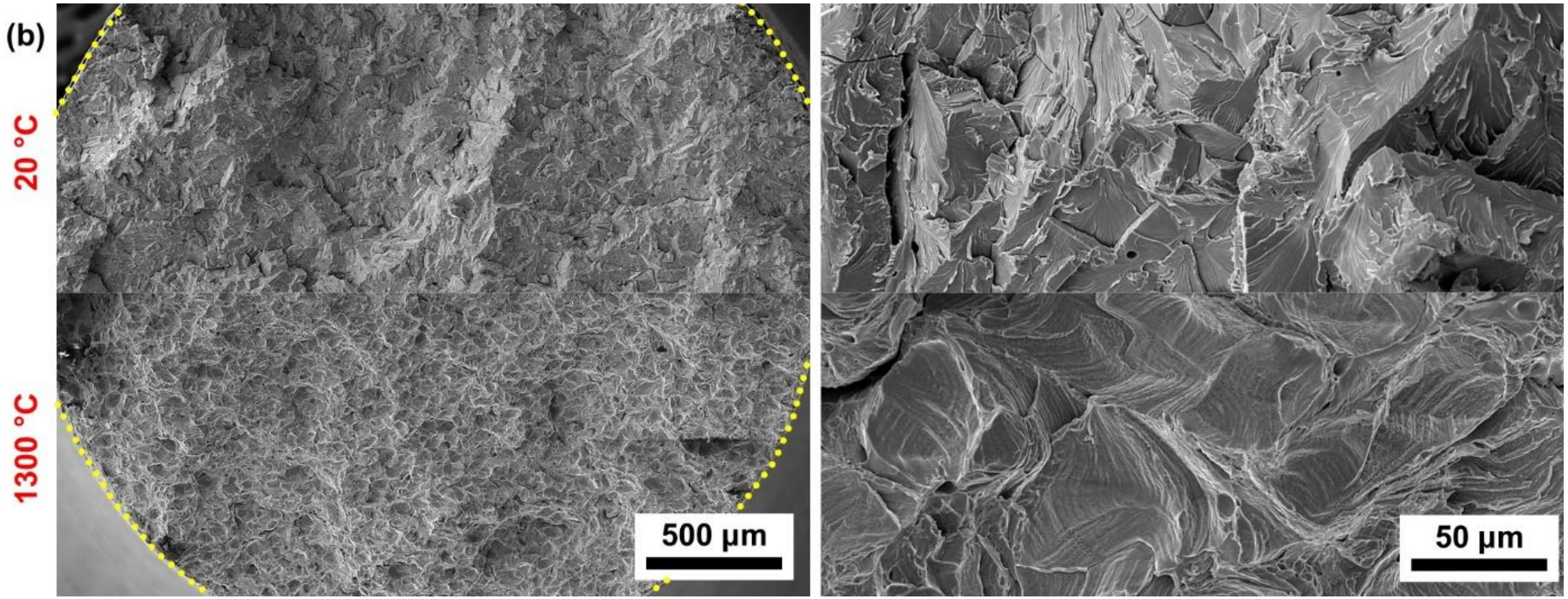

Low (200 X) and high (2 kX) magnification secondary electron images

Fractography

- Fracture regions outlined in a yellow-dotted line

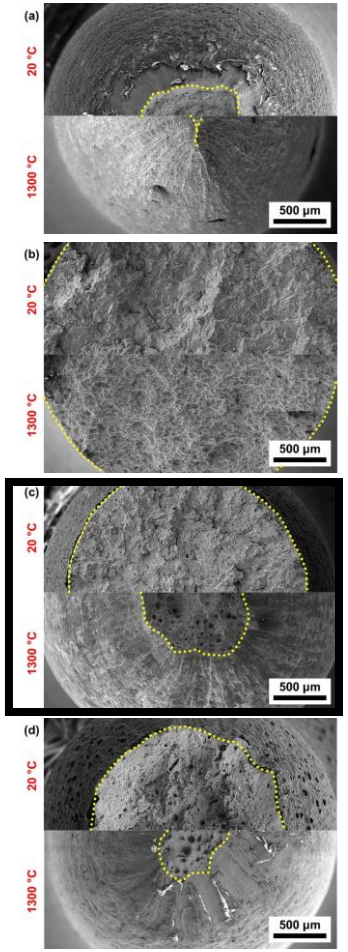

Nb-1ZrC

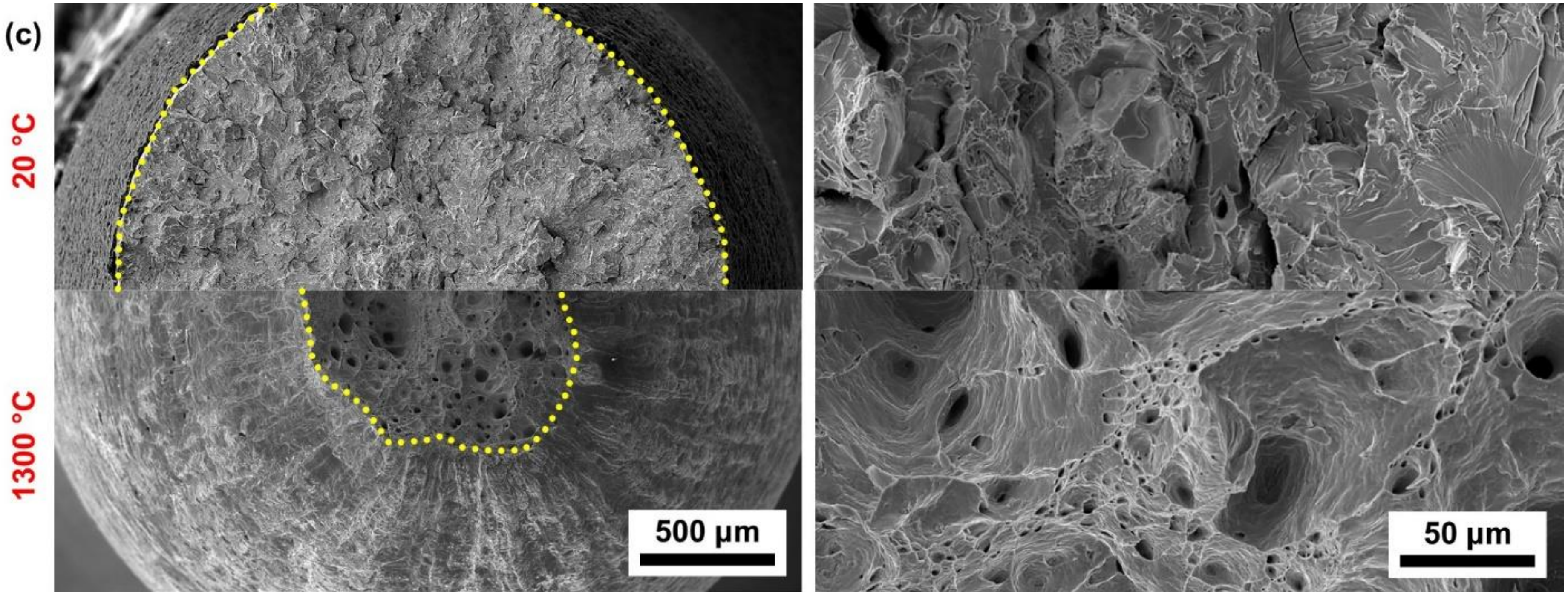

Low (200 X) and high (2 kX) magnification secondary electron images

Fractography

- Fracture regions outlined in a yellow-dotted line

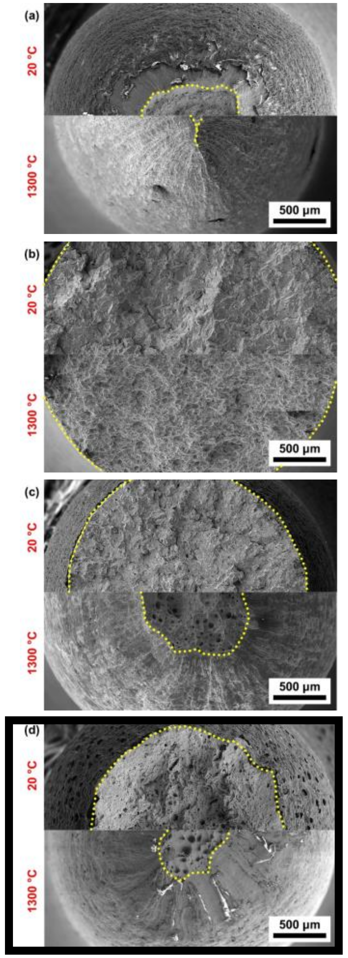

Nb-1ZrH$_2$

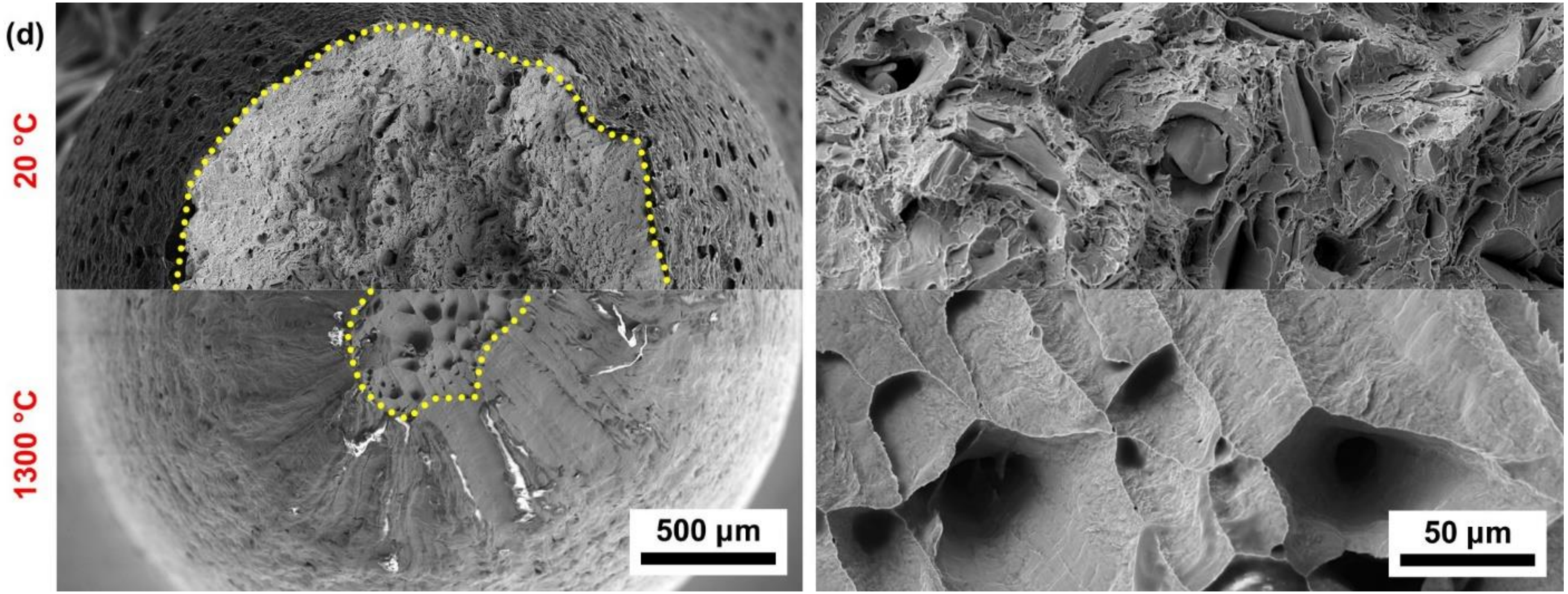

Low (200 X) and high (2 kX) magnification secondary electron images

Microstructural Characterization - SEM

- Wrought: significant grain growth, no precipitates

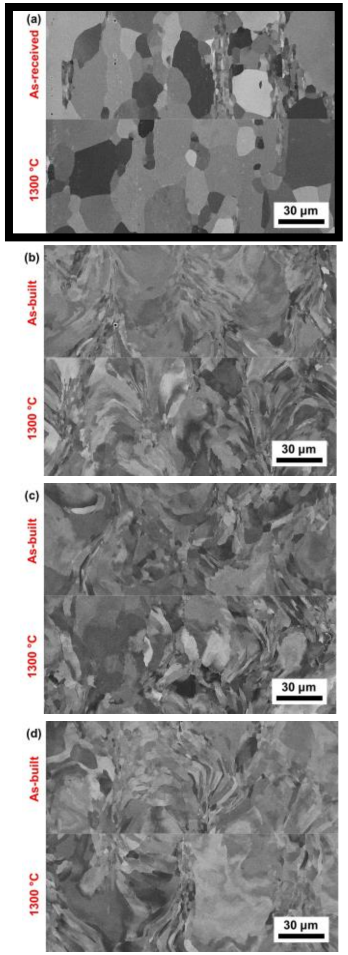

Wrought

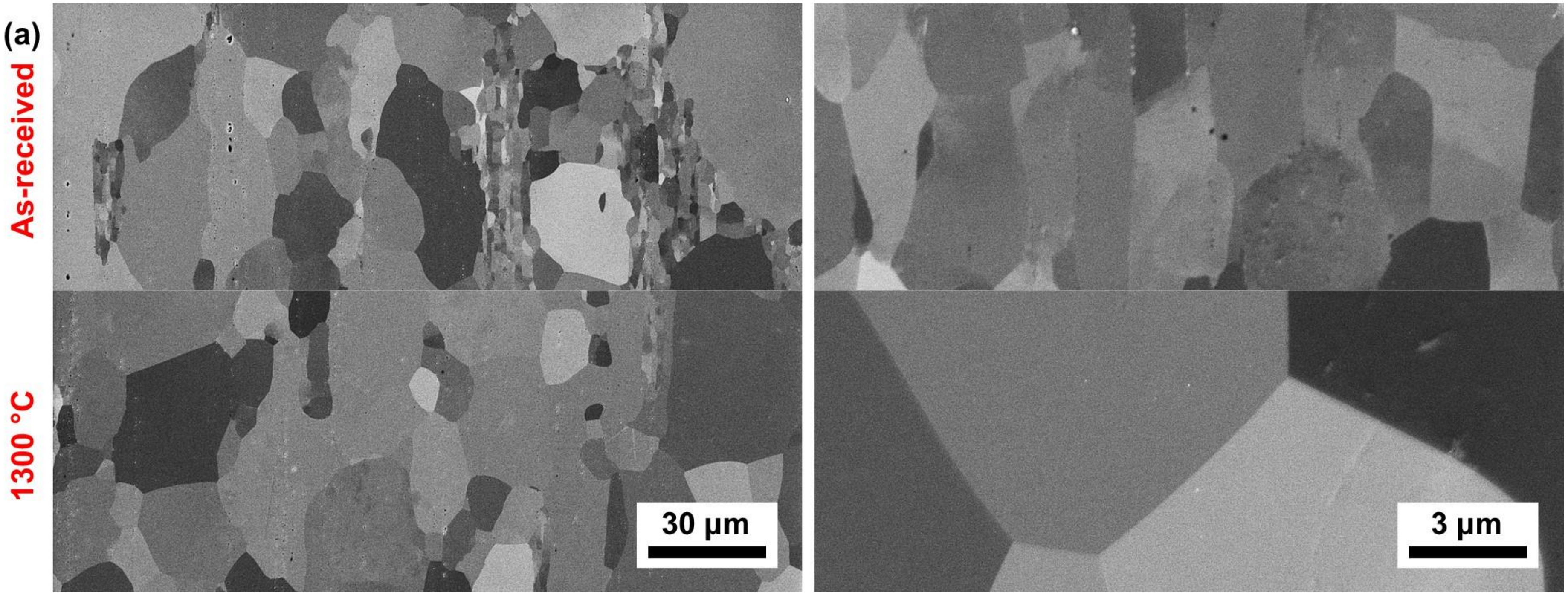

Low (3 kX) and high (30 kX) magnification secondary electron images

Microstructural Characterization - SEM

- Nb-1ZrO_2: no grain growth, no precipitates

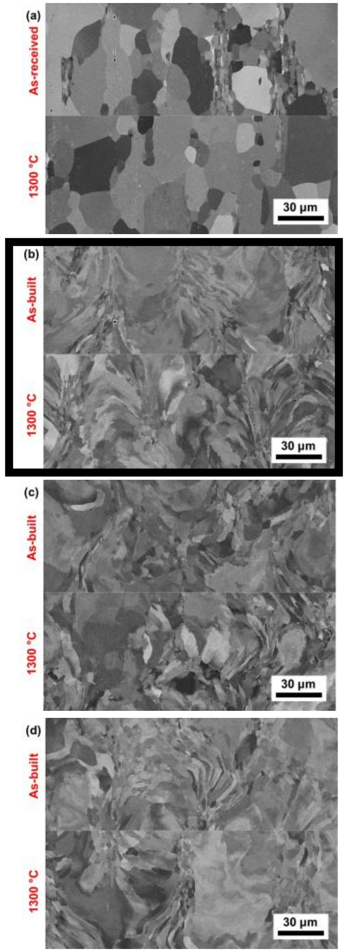

Nb-1ZrO_2

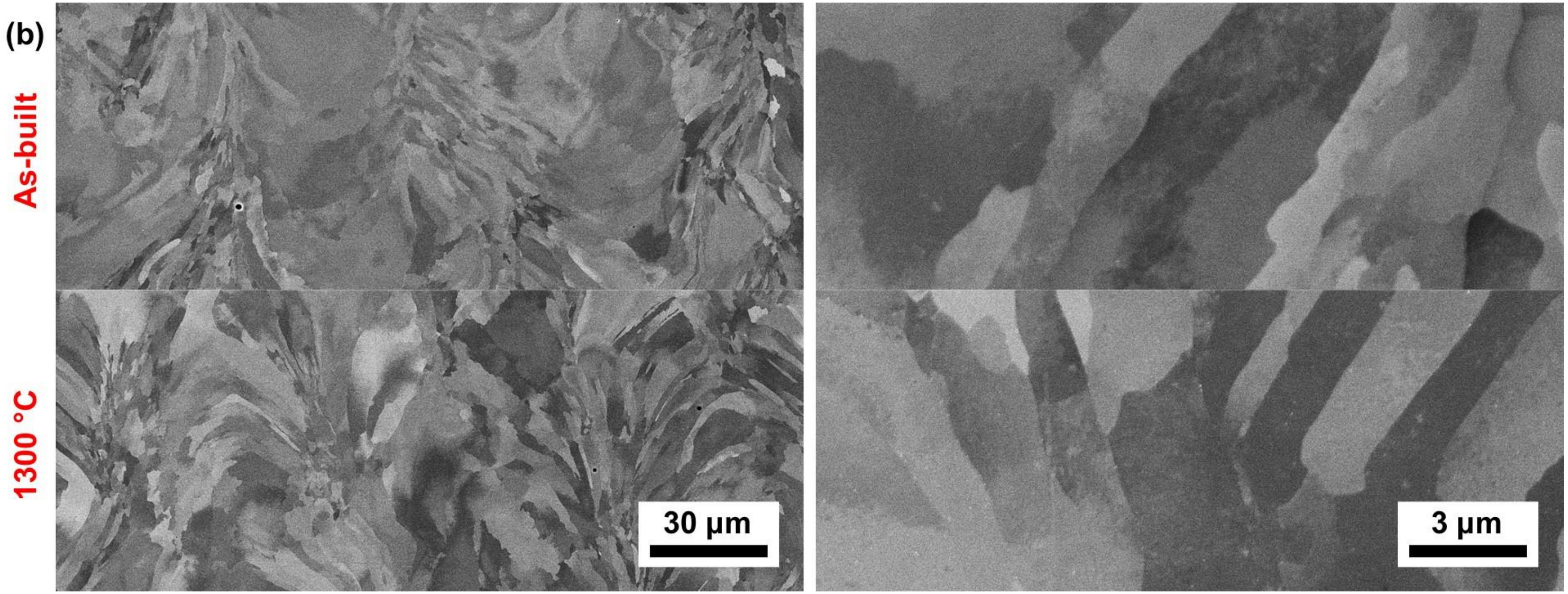

Low (3 kX) and high (30 kX) magnification secondary electron images

Microstructural Characterization - SEM

- Nb-1ZrC: no grain growth, precipitates at grain boundaries and within grains

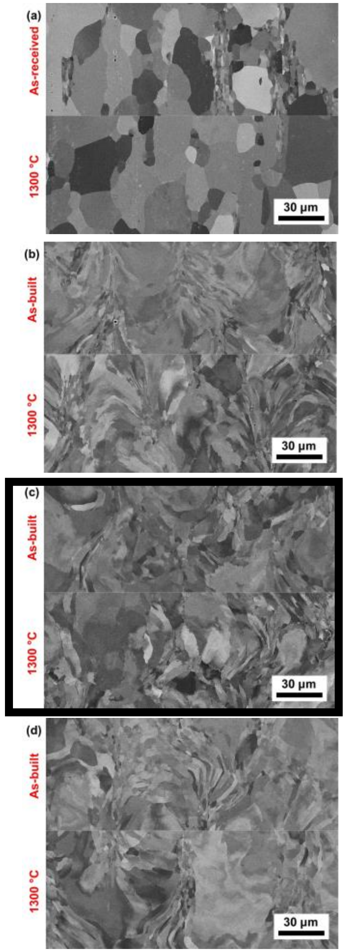

Nb-1ZrC

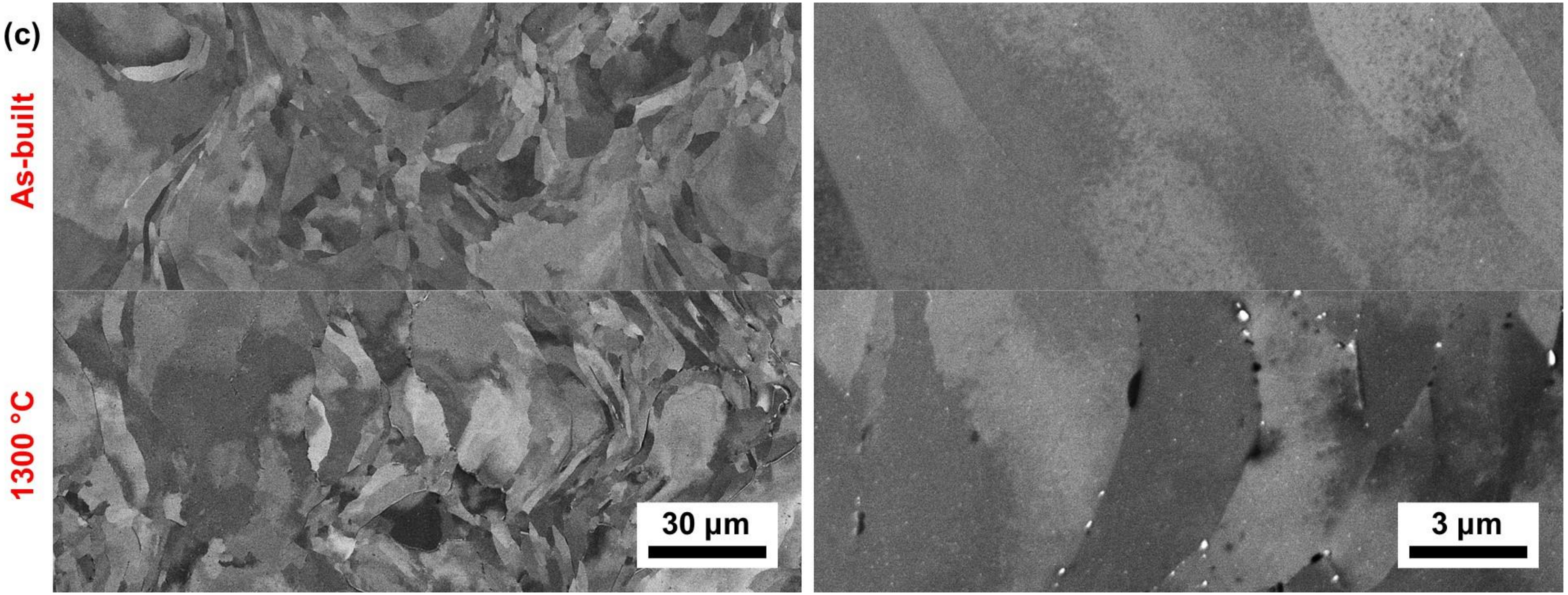

Low (3 kX) and high (30 kX) magnification secondary electron images

Microstructural Characterization - SEM

- $Nb\text{-}1ZrH_2$: no grain growth, precipitates at grain boundaries and within grains

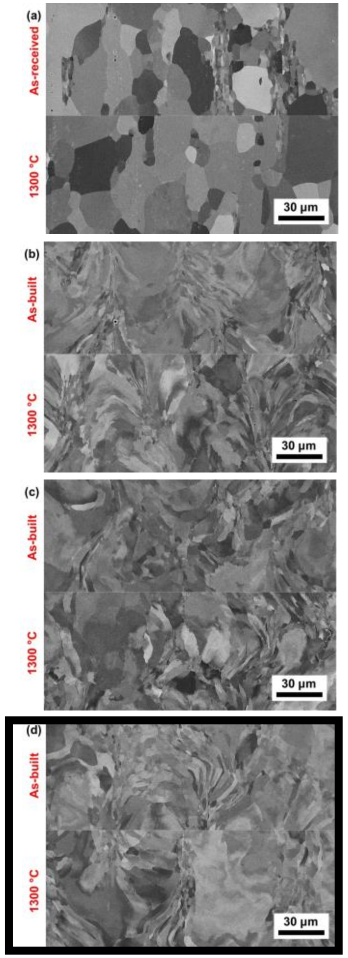

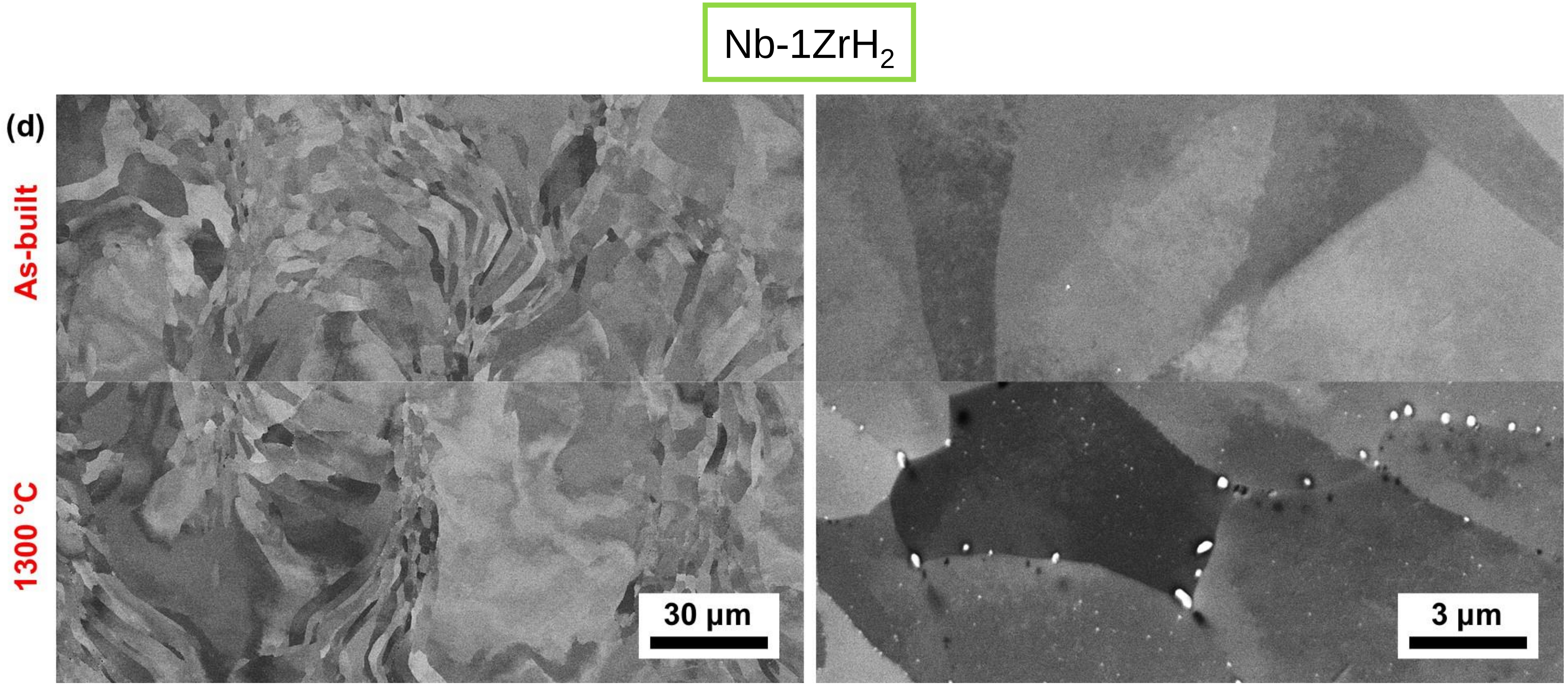

Low (3 kX) and high (30 kX) magnification secondary electron images

Microstructural Characterization – SEM/EDS

- Grain boundary precipitates identified as zirconium oxides

$Nb\text{-}1ZrH_2$

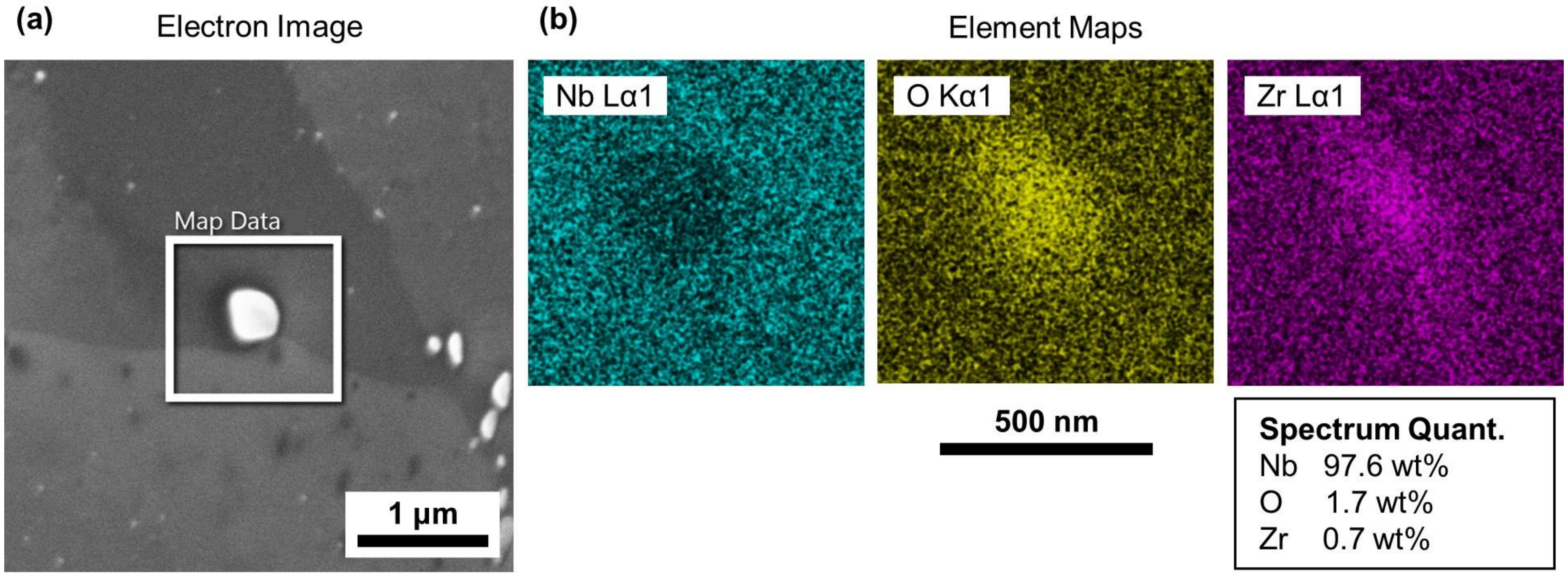

50 kX magnification secondary electron image

Microstructural Characterization – EBSD of As-built

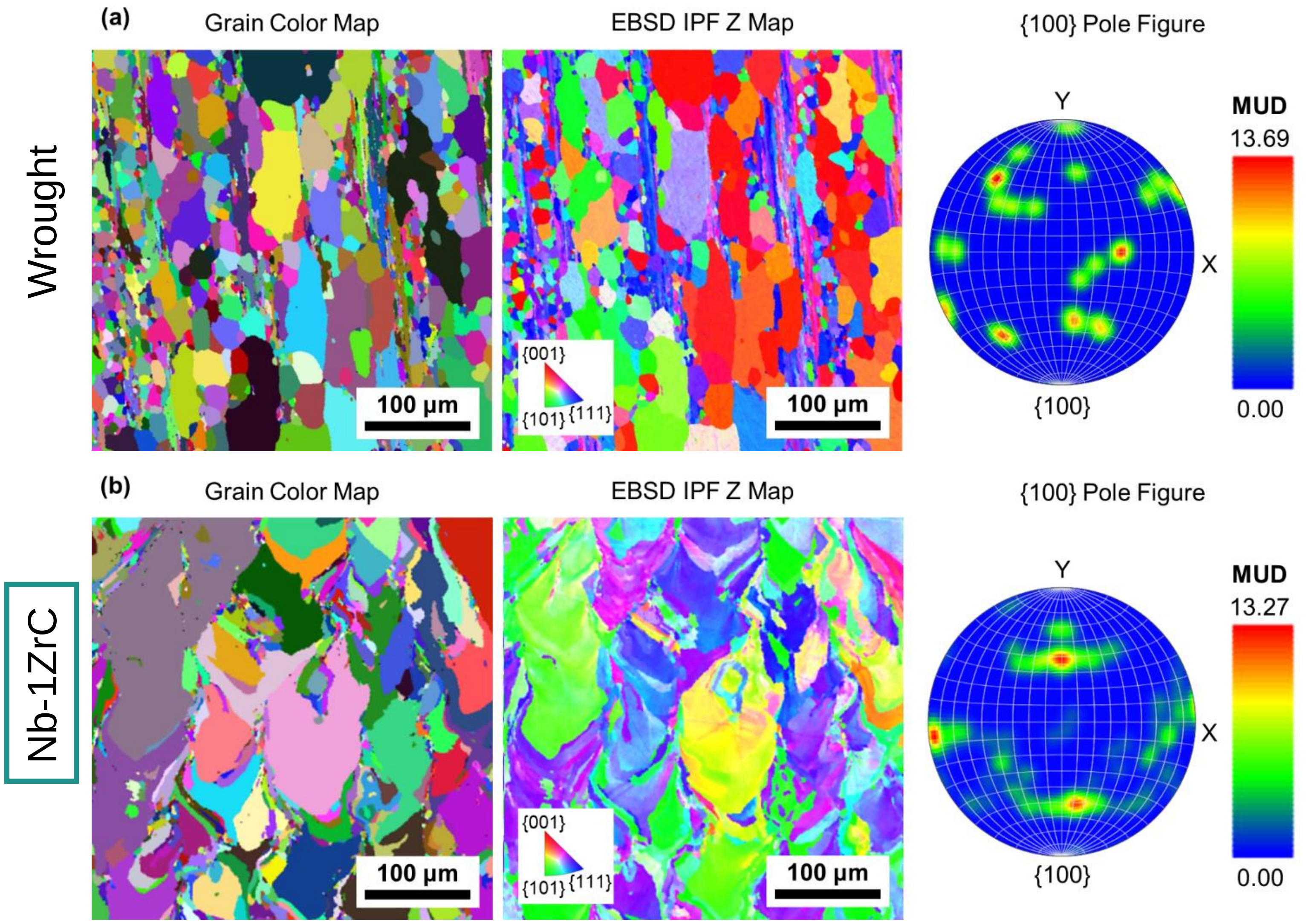

Microstructural Characterization – EBSD of As-built

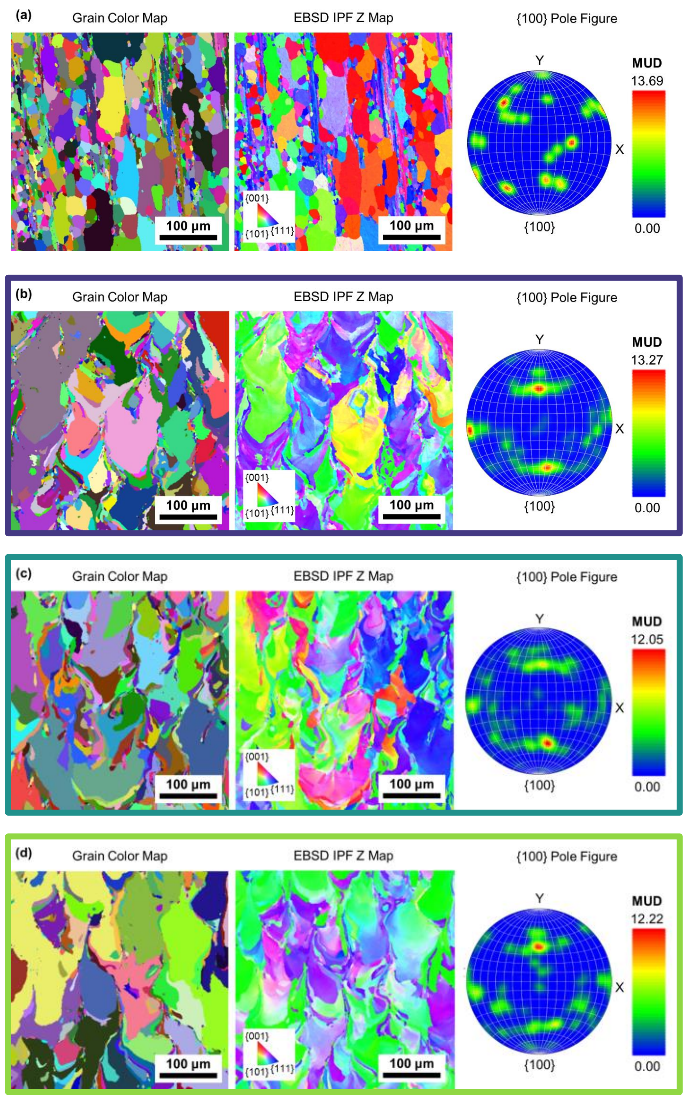

Material	EBSD Grain Statistics (Average)				
	ECD [µm]	Length [µm]	Aspect Ratio	GOS [°]	MOS [°]
Wrought	6.20	10.62	2.13	0.97	2.37
Nb-1ZrO_2	6.00	11.18	2.15	1.27	2.82
Nb-1ZrC	7.37	14.43	2.43	1.20	2.93
Nb-1ZrH_2	7.51	15.00	2.49	1.07	2.49

Average EBSD grain statistics for the wrought and L-PBF consolidated niobium materials

Conclusions

1. The ZrH_2 addition achieved the greatest L-PBF relative density compared to the ZrC and ZrO_2 (99.89 % > 99.75 % > 99.65 %)
2. 1 wt% addition of ZrH_2 was sufficient to produce a Zr alloy content within ASTM B391 specification (0.83 wt%)
3. The printed Nb-1ZrH_2 material exhibited room temperature hammer-bend test performance similar to wrought Nb-1Zr
4. The ZrO_2 addition offered the greatest elevated temperature strength; however, the material suffered from brittle behavior with ductility (< 6-7 %)
5. Both ZrC and ZrH_2 modified feedstocks showed ductile fracture features, especially at 1300°C
6. The Nb-1ZrO_2 material did not form grain boundary precipitates during the 1300°C exposure, and had the finest as-built L-PBF microstructure with grain ECD and aspect ratio comparable to the wrought Nb-1Zr